Sensitivity of cavity optomechanical field sensors

J. Knittel[a], S. Forstner[a,b], J. D. Swaim[a], H. Rubinsztein-Dunlop[a], and W. P. Bowen[a]

[a]School of Mathematics and Physics, University of Queensland, St Lucia, Queensland 4072, Australia;
[b]Physik-Department, TU Muenchen, 85748 Garching, Germany

ABSTRACT

This article presents a technique for modeling cavity optomechanical field sensors. A magnetic or electric field induces a spatially varying strain across the sensor. The effect of this strain is accounted for by separating the mechanical motion of the sensor into eigenmodes, each modeled by a simple harmonic oscillator. The force induced on each oscillator can then be determined from an overlap integral between strain and the corresponding eigenmode, with the optomechanical coupling strength determining the ultimate resolution with which this force can be detected.

Keywords: cavity optomechanics, magnetic field sensors, magnetostriction, integrated microcavity

1. INTRODUCTION

Today, ultra-sensitive field sensors, and most particularly magnetometers, play important roles in a diverse range of fields including geology, mineral exploration, archaeology, material-testing and medicine.[1] Thus many different types of magnetometer have been developed taking advantage of a range of different physical phenomena[1,2] including giant magnetoresistance in thin films,[3] magnetostriction,[4] magnetic force microscopy,[5] quantum interference in superconductors,[6] the Hall effect,[7] optical pumping,[8] electron spin resonances in solids[9] and even Bose-Einstein condensation.[10] Currently, the most practical and widely used ultra-low field magnetometer is based on the superconducting quantum interference device (SQUID),[11] where the magnetic field induces a current in a superconducting loop containing Josephson-junctions. These magnetometers achieve sensitivities as good as 1 fT Hz$^{-1/2}$,[1] enabling SQUIDs to detect single flux quanta. However, SQUIDs require cryogenic cooling, which increases operational costs and complicates applications.[12] Hence, significant research effort has been put into implementing ultrasensitive magnetometers able to operate at room temperature. Magnetic field measurements with record sensitivities of 160 aT Hz$^{-1/2}$ at room temperature are possible with spin exchange relaxation-free (SERF) magnetometers.[8] SERFs have been used successfully in various applications including medicine and geology. However, they are limited to mm size scales even when using microfabricated gas cells,[13] and have low dynamic range due to the non-linear Zeeman effect which is significant even at geomagnetic field strengths ($\approx 50\mu T$)[11,14]

NV center based magnetometers overcome the size constraint, being nm to μm size. They allow sensitivities as good as 3 nT Hz$^{-1/2}$ at room temperature,[15] and magnetic field imaging[16] and magnetic resonance imaging[17] at the nanoscale. Theoretical modelling predicts that sensitivities as in the fT Hz$^{-1/2}$ range may be possible[16] with such devices. However, NV centre based magnetometers have some constraints, including sensitivity to magnetic field misalignment,[18] complexity of magnetic field readout,[19] and the requirement of bulky optics.

Many applications require a sensor of small geometric dimensions combined with high sensitivity. For example in low field nuclear magnetic resonance imaging,[20,21] the sensitivity of the instruments can be enhanced by placing the magnetic field sensor close to the sample. This also applies to investigations in the field of solid state physics and superconductivity.[22,23] It is even more relevant for measurements of single dipole moments, as the magnetic dipole-field decays with the distance r as $1/r^3$. In medical applications, richer diagnostic information is obtained by imaging the magnetic field distribution with the highest possible resolution and sensitivity. For example Magneto-cardiography(MCG),[1,14] the imaging of the magnetic fields generated by the human heart, relies on

---

Further author information: (Send correspondence to W.P.B.)
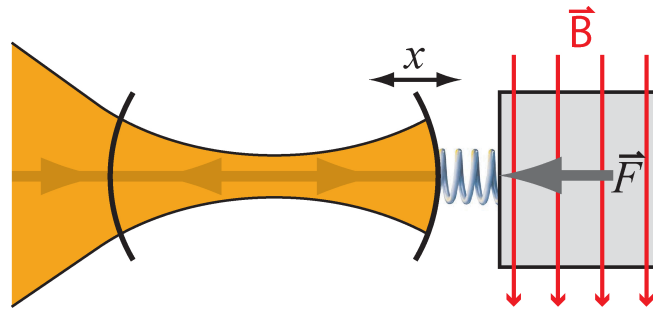W.P.B.: E-mail: w.bowen@uq.edu.au, Telephone: 61 7 3346 9425

Figure 1. A cavity optomechanical field sensor, illustrated via the example of a Fabry-Perot-type cavity with a harmonic spring attached to one of the mirrors. A field sensitive medium responds to an external field, applying a force on the spring and causing a displacement of the mirror. A mirror displacement results in a change in the optical path length, modifying the resonance frequency of the cavity. For sensing applications, we assume that the radiation pressure force has negligible effect on the cavity resonance frequency.

signals in the low pT-range. The fields generated by the neurons in the human brain are even weaker with flux densities between 10fT (for the celebral cortex[24]) and 1 pT (for synchronous and coherent activity of the thalamic pacemaker cells, resulting in α-rhythm[25]). The imaging of these fields requires highly sensitive magnetometers with high spatial and temporal resolution.[24] Thus, multiple sensors in a dense 2-dimensional array with simple readout and uncomplicated handling are desirable to measure magnetic field distributions with good spatial resolution.

Recently, a new form of field sensor has been demonstrated based on cavity optomechanical systems,[26] where the cavity optical resonance frequencies are coupled to the mechanical deformation of the cavity structure as depicted in Fig. 1. The cavity optomechanical system is functionalized by attachment of a material which responds mechanically to an applied field, which could be, for example, an electric or a magnetic field. The response of the material to the applied field then stresses the mechanical structure of the cavity, resulting in a shift in its optical resonance frequencies which can be readout using an optical field giving a measurement of the applied field. By engineering both high quality mechanical vibrations in the mechanical structure and high optical quality resonances in the optical cavity, the sensitivity of the measurement is doubly enhanced. The magnetometer demonstrated in Ref.[26] was based on lithographically fabricated optical microtoroidal resonators coupled to the magnetostrictive material Terfenol-D. The lithographic fabrication and fiber or waveguide coupling offers the potential for arrays of sensors; high quality optical and mechanical resonances are present in microtoroids; and Terfenol-D stretches signifcantly at room temperature under applied magnetic fields. Sensitivities in the range of one hundred nT Hz$^{-1/2}$ were demonstrated based on this construction, with theoretical sensitivities in the pT Hz$^{-1/2}$ range predicted for an optimized geometry.[26] Here, we extend the theoretical model in Ref.,[26] presenting an eigenmode based method for calculation of the predicted sensitivity of general cavity opto-mechanical field sensors.

2. THE CONCEPT OF A CAVITY OPTOMECHANICAL FIELD SENSOR

The field of cavity optomechanics results from the coalescence of two previously separate areas of research, optical microcavities and mechanical microresonators.[27] Light acts on mechanical degrees of freedom via radiation pressure. This aspect of optomechanics has been subject to intense research in the past decades, and has first been experimentally described in large-scale interferometric gravitational wave experiments.[28] Reciprocally, mechanical displacements x act on optical degrees of freedom, as they modify the optical path length, manifest as a measurable change in the cavities resonance frequency. In a high quality optical microcavity this change in cavity resonance frequency can be detected via an in-coupled optical field with high precision, allowing mechanical displacement to be measured with accuracy as good as 10^{-19} m Hz$^{-1/2}$.[29,30] Since applied forces cause mechanical displacements, this capacity to measure displacements with high precision provides COMS with the potential to achieve sensitive force measurement. However, as force sensors, COMS are generally outperformed by nano-electromechanical systems (NEMS), i.e. NEMS cantilevers.[31] The extremely low mass of

NEMS makes them receptive to minute forces. Cavity optomechanical systems (COMS) have a larger mass and thus seem to be less suited for these applications. However, in field sensing the larger volume of COMS increases the coupling to external fields and makes COMS potentially competitive for ultra-low field sensing applications.

Microtoroids, as discussed earlier, are prominent representatives of COMS. Other actively researched COMS include photonic crystal cavities,[32, 33] nanomembranes made from GaAs[34] or SiN,[35] ZnO-microwires,[36] and many others.[37–39]

3. FORCE AND FIELD SENSITIVITY OF A GENERAL OPTOMECHANICAL SENSOR

3.1 Eigenmodes

The mechanical motion of a COMS can be decomposed into its intrinsic vibrational eigenmodes, allowing the system to be described as a set of damped harmonic oscillators. In an isotropic homogeneous medium, the equation of motion for the mechanical vibration is given by the elastic wave equation[40]

$$\rho\ddot{\vec{u}}(\vec{r},t) = (\lambda + \mu)\vec{\nabla}(\vec{\nabla}\cdot\vec{u}(\vec{r},t)) + \mu\vec{\nabla}^2\vec{u}(\vec{r},t), \tag{1}$$

where the vector field $u(\vec{r},t)$ denotes the displacement of an infinitesimally small cubic volume element at initial position $\vec{r}$ and time t, and λ and μ are the Lamé-constants

$$\lambda = \frac{\sigma E}{(1+\sigma)(1-2\sigma)} \tag{2}$$

$$\mu = \frac{E}{2(1+\sigma)} \tag{3}$$

with σ and E being Poisson's ratio and Young's modulus, respectively.

It is well known that a complete set of orthonormal eigenmode solutions can be found for Eq. (1) by looking for solutions with separable spatially and temporally varying parts of the form

$$\vec{u}(\vec{r},t) = \vec{\Psi}_q(\vec{r})X_q(t), \tag{4}$$

where $X_q(t)$ is the time dependent oscillation of eigenmode q and $\vec{\Psi}_q(\vec{r})$ is it's position dependent modeshape function, normalized such that $\int_V \vec{\Psi}_p(\vec{r})\cdot\vec{\Psi}_q(\vec{r})d^3r = V\delta_{pq}$ with V being the spatial volume of the oscillator. When inserted into Eq. (1) this yields the new equation of motion

$$\ddot{X}_q(t) = \left[\frac{(\lambda+\mu)\vec{\nabla}(\vec{\nabla}\cdot\vec{\Psi}_q(\vec{r})) + \mu\vec{\nabla}^2\vec{\Psi}_q(\vec{r})}{\rho\vec{\Psi}_q(\vec{r})}\right]X_q(t) \tag{5}$$

Since the left hand side of this equation is evidently independent of position $\vec{r}$, so must be the right hand side, with the term in square brackets being constant and causing the elastic restoring force of the material. For the mechanical motion to be stable, this term must also be negative, and with the benefit of hindsight, we define it to equal $-\omega_q^2$ here. The equation of motion is then separable into one spatial and one temporal equation of motion

$$(\lambda+\mu)\vec{\nabla}(\vec{\nabla}\cdot\vec{\Psi}_q(\vec{r}) + \mu\vec{\nabla}^2\vec{\Psi}_q(\vec{r})) = -\rho\omega_q^2\vec{\Psi}_q(\vec{r}) \tag{6}$$

$$\ddot{X}_q(t) = -\omega_q^2 X_q(t). \tag{7}$$

The second equation here is, of course, just Hookes law for an oscillator with resonance frequency ω_q and spring constant $k_q = M\omega_q^2$, where M is the mass of the oscillator. Hence, as expected, the elastic nature of the material causes the amplitude of each eigenmode to independently oscillate at a characteristic frequency just like a mass on a spring. Solving the first equation for the spatial eigenmodes of vibration is generally difficult and in many cases only numerical solutions are possible, however the solution yields a complete set of orthogonal eigenmodes each with a characteristic value for ω_q specified by $\omega_q^2 = -\left[(\lambda+\mu)\vec{\nabla}(\vec{\nabla}\cdot\vec{\Psi}_q(\vec{r})) + \mu\vec{\nabla}^2\vec{\Psi}_q(\vec{r})\right]/\rho\vec{\Psi}_q(\vec{r})$. The total displacement vector field $u(\vec{r},t)$ for a general motion of the oscillator can of course be expanded as

$$\vec{u}(\vec{r},t) = \sum_q \vec{u}_q(\vec{r},t) = \sum_q X_q(t)\vec{\Psi}_q(\vec{r}). \tag{8}$$

3.2 Including external forces and dissipation

Let us now consider the response of the mechanical modes to a force density $\vec{f}(\vec{r}, t)$ applied to the mechanical structure. Including this force density, the elastic wave equation [Eq. (1)] becomes

$$\rho \ddot{\vec{u}}(\vec{r}, t) = (\lambda + \mu)\vec{\nabla}(\vec{\nabla} \cdot \vec{u}(\vec{r}, t)) + \mu \vec{\nabla}^2 \vec{u}(\vec{r}, t) + \vec{f}(\vec{r}, t) \tag{9}$$

As with the mechanical motion, the force density can be expressed in terms of a set of eigenmodes with each separable into temporally and spatially varying components

$$\vec{f}(\vec{r}, t) = \frac{1}{V} \sum_q F_q(t) \vec{\Psi}_q(\vec{r}) \tag{10}$$

where $F_q(t)$ is the force in Newtons acting on mechanical eigenmode q. Substituting this expression into Eq. (9) along with the mode expansion for $\vec{u}(\vec{r}, t)$ given in Eq. (8), multiplying the resulting expression on both sides by $\vec{\Psi}_p$, and integrating over the volume of the mechanical oscillator yields independent equations of motion for each mechanical mode

$$M\left[\ddot{X}_q(t) + \Gamma_q \dot{X}_q(t) + \omega_q^2 X_q(t)\right] = F_q(t), \tag{11}$$

where we have made use of the fact that $M = \rho V$ and the orthonormality condition $\int_V \vec{\Psi}_q(\vec{r}) \cdot \vec{\Psi}_p(\vec{r}) d^3 r = V\delta_{qp}$, and have introduced independent linear decay with rate Γ_q to each of the mechanical eigenmodes as is typical of damping in mechanical oscillators.

The force $F_n(t)$ can contain forces from a range of different sources. The three forces relevant to this article are the Brownian noise force $F_{\text{th},q}(t)$, the radiation pressure force from the presence of the optical field used to monitor the mechanical motion $F_{\text{rp},q}(t)$, and the force applied by the signal field which we aim to detect $F_{\text{sig},q}(t)$; with the total force $F_q(t) = F_{\text{th},q}(t) + F_{\text{rp},q}(t) + F_{\text{sig},q}(t)$. The thermal force can be shown from the fluctuation-dissipation theorem to equal

$$F_{\text{th},q}(t) = \sqrt{2M\Gamma_q k_B T}\xi_q(t), \tag{12}$$

where $k_B = 1.381$ m^2 kg s^{-1} K^{-1} is the Boltzmann-constant, T is the temperature of the system, and $\xi_q(t)$ is a unit white noise Wiener process. The radiation pressure force, and complimentary frequency shift on the optical mode $\delta\Omega_q$ can be determined from Hamiltonian mechanics using the optomechanical interaction Hamiltonian $H_{I,q} = \hbar G_q X_q(t) n(t)$, where $n(t)$ is the number of photons within the optical resonator and $G_q = d\Omega_q/dX_q$ is the optomechanical coupling strength with Ω being the optical resonance frequency.[41] The result is

$$F_{\text{rp},q}(t) = \hbar G_q n(t) \tag{13}$$
$$\delta\Omega_q = G_q X_q(t). \tag{14}$$

Hence, the equation of motion for mechanical mode q can be expressed as

$$M\left[\ddot{X}_q(t) + \Gamma_q \dot{X}_q(t) + \omega_q^2 X_q(t)\right] = \sqrt{2M\Gamma_q k_B T}\xi_q(t) + \hbar G_q n(t) + F_{\text{sig},q}(t). \tag{15}$$

3.3 Conversion to measurable parameters

The equation above completely describes the motion of the qth mechanical eigenmode of the oscillator. However, in general the displacement parameter $X_q(t)$ may not be directly accessible. In the case of optical measurement considered here, the measured signal is the frequency shift on the optical mode, which provides the change in optical path length x rather than $X_q(t)$. Hence, to apply Eq. (15) to optical measurements made in a cavity optomechanical system the length coordinate must be rescaled in terms of this measured variable. Furthermore, since the optomechanical coupling rate is defined in terms of the optical resonance frequency shift for a given displacement of the mechanical oscillator, the use of a different length scale results in a modification to this rate. The raw optomechanical coupling rate G_q, must therefore also be replaced with the measurable optomechanical coupling rate g_q. The purpose of this section is to mathematically perform the transformation to these measurable parameters.

To rescale the position coordinate, we recognize that the optomechanical interaction energy must remain constant under a change in coordinate system, so that $H_{I,q} = \hbar G_q X_q(t)n(t) = \hbar g_q x_q(t)n(t)$, where $g_q = d\Omega_q/dx_q$ is the directly measurable optomechanical coupling strength in the new optically defined coordinate system. Consequently,

$$X_q(t) = \frac{g_q}{G_q} x_q(t). \tag{16}$$

Similarly, since the potential energy of the mechanical mode U_q must be constant under the co-ordinate transformation we have

$$U_q = \frac{1}{2} M \omega_q^2 X_q^2(t) = \frac{1}{2} m_q \omega_q^2 x_q^2(t), \tag{17}$$

where the modified *effective mass* of the eigenmode m_q naturally arises from the change in length scale, with the ratio of total to effective masses given by

$$\frac{M}{m_q} = \left(\frac{x_q}{X_q}\right)^2 = \left(\frac{G_q}{g_q}\right)^2. \tag{18}$$

Rearranging we find

$$G_q = g_q \sqrt{\frac{M}{m_q}}. \tag{19}$$

Substituting for $X_q(t)$ and G_q in Eq. (15) an equation of motion for the mechanical oscillator eigenmodes in terms of measurable parameters is finally obtained

$$m_q \left[\ddot{x}_q(t) + \Gamma_q \dot{x}_q(t) + \omega_q^2 x_q(t)\right] = \sqrt{2 m_q \Gamma_q k_B T} \xi_q(t) + \hbar g_q n(t) + \sqrt{\frac{m_q}{M}} F_{\text{sig},q}(t). \tag{20}$$

This equation of motion is identical in form to the unscaled equation of motion, except for a scaling of the signal force caused by the modification of effective mass.

3.4 Force and field sensitivity

To determine the sensitivity of the cavity optomechanical sensor we start by solving Eq. (20) in the frequency domain. Taking the Fourier transform we find

$$x_q(\omega) = \chi_q(\omega) \left[\sqrt{2 m_q \Gamma_q k_B T} \xi_q(\omega) + \hbar g_q n(\omega) + \sqrt{\frac{m_q}{M}} F_{\text{sig},q}(\omega)\right], \tag{21}$$

where $\chi_q = [m_q(\omega_q^2 - \omega^2 - i\Gamma_q \omega)]^{-1}$ is the susceptibility of the mechanical mode. As mentioned before, this causes an observable shift in the resonance frequency of the optical resonator. The magnitude can be determined from Eqs. (14) and (16) as $\delta\Omega_q = g_q x_q(t)$, so that in the frequency domain

$$\delta\Omega_q(\omega) = g_q \chi_q(\omega) \left[\sqrt{2 m_q \Gamma_q k_B T} \xi_q(\omega) + \hbar g_q n(\omega) + \sqrt{\frac{m_q}{M}} F_{\text{sig},q}(\omega)\right]. \tag{22}$$

The spectral power contributions from signal $S_{\Omega\Omega}^{\text{sig},q}$ and noise $S_{\Omega\Omega}^{\text{noise},q}$ in the final detected signal can then be calculated as

$$S_{\Omega\Omega}^{\text{sig},q} = |\langle \delta\Omega_q(\omega)\rangle|^2 \tag{23}$$

$$S_{\Omega\Omega}^{\text{noise},q} = \langle|\delta\Omega_q(\omega)|^2\rangle - |\langle\delta\Omega_q(\omega)\rangle|^2 + S_{\Omega\Omega}^{\text{meas}}(\omega), \tag{24}$$

where we have included the measurement noise term $S_{\Omega\Omega}^{\text{meas}}(\omega)$ which accounts for shot and frequency noise on the laser field, and other noise sources such as electronic noise in the detectors used to measure the optical field. Taking a signal force $F_{\text{sig},q}(\omega) = F_{\text{sig},q}\delta(\omega - \omega_{\text{sig}})$ at the single frequency ω_{sig}, we find

$$S_{\Omega\Omega}^{\text{sig},q} = g_q^2 |\chi_q(\omega)|^2 \frac{m_q}{M} F_{\text{sig},q}^2 \delta(\omega - \omega_{\text{sig}}) \tag{25}$$

$$S_{\Omega\Omega}^{\text{noise},q} = g_q^2 |\chi_q(\omega)|^2 \left[2 m_q \Gamma_q k_B T + \hbar^2 g_q^2 \langle\delta n(\omega)^2\rangle\right] + S_{\Omega\Omega}^{\text{meas},q}(\omega), \tag{26}$$

where we have used the fact that $\xi_q(t)$ is unit white noise such that $\langle|\xi_q(t)|^2\rangle = 1$, and $\delta n(\omega) = n(\omega) - \langle n(\omega)\rangle$ denotes the fluctuations in the photon number within the optical resonator.

The minimum detectable force $F_{\text{sig},q}^{\text{min}}$ is obtained by integrating signal and noise contributions over the bandwidth of the measuring system $\Delta\omega$ and setting the signal and noise powers equal such that the signal-to-noise ratio is unity

$$\frac{F_{\text{sig},q}^{\text{min}}}{\sqrt{\Delta\omega}} = \sqrt{2M\Gamma_q k_B T + \frac{M}{m_q}\left[\hbar^2 g_q^2\langle\delta n(\omega)^2\rangle + \frac{S_{\Omega\Omega}^{\text{meas},q}}{g_q^2|\chi_q(\omega)|^2}\right]}. \tag{27}$$

In order to determine the sensitivity to an applied spatially uniform field $\vec{\Phi}(t) = \vec{\Phi}e^{i\omega_{\text{sig}}t}$, the body force density $\vec{f}_{\text{sig}}(\vec{r},t)$ due to the applied field must be determined. This can be achieved via finite element modeling. The force on a specific mechanical eigenmode can then be found via

$$F_{\text{sig},q}(t) = \int_V \vec{\Psi}_q(\vec{r}) \cdot \vec{f}_{\text{sig}}(\vec{r},t)d^3r, \tag{28}$$

which can be easily derived from Eq. (10) and the orthonormality relation for mechanical eigenmodes. In typical circumstances, a linear relationship will exist between this force and the amplitude of the applied field, such that $F_{\text{sig},q} = c_{\text{act},q}|\vec{\Phi}|$, where the *actuation constant* $c_{\text{act},q}$, determines the strength of the coupling and can be found via the finite element model. The minimum detectable field is then simply found by substituting this relationship into Eq. (27)

$$\frac{|\vec{\Phi}_q|^{\text{min}}}{\sqrt{\Delta\omega}} = \frac{1}{c_{\text{act},q}}\sqrt{2M\Gamma_q kT + \frac{M}{m_q}\left[\hbar^2 g_q^2\langle\delta n(\omega)^2\rangle + \frac{S_{\Omega\Omega}^{\text{meas},q}}{g_q^2|\chi_q(\omega)|^2}\right]}. \tag{29}$$

It can be seen that, in the usual limit where the radiation pressure force due to photon number fluctuations is negligible, high mechanical quality factor (i.e. low damping rate Γ_q) is always advantageous for precise sensing, reducing the thermal noise, and also, on resonance, the effect of the measurement noise through its contribution to the mechanical susceptibility $\chi_q(\omega)$.

A similar approach to that presented here has be followed in Ref.[26] to determine the sensitivity of a microtoroid based magnetometer sensitized to magnetic fields via attached of a magnetostrictive material, predicting sensitivities in the pico-Tesla per root Hertz range.

4. CONCLUSION

We have presented a technique to predict the sensitivity of cavity optomechanical field sensors. This technique could be used to optimize the design of these sensors. Cavity optomechanical field sensors are particularly attractive as magnetometers, with sensitivities in the range of nano-Telsa per root Hertz already demonstrated in a recent experiment.[26]

REFERENCES

[1] A. Edelstein. Advances in magnetometry. *Journal of Physics: Condensed Matter,* 19, 28 (2007).

[2] M. Diaz-Michelena. Small Magnetic Sensors for Space Applications. *Sensors,* 9, 2271 (2009).

[3] P. Ripka, and M. Janosek. Advances in Magnetic Field Sensors *IEEE Sensors Journal,* 10, 1108 (2010).

[4] F. Bucholtz, D. M. Dagenais, and K. P. Koo. High-frequency fibre-optic magnetometer with 70 $fT/\sqrt{Hz}$ resolution. *Electronics Letters,* 25, 1719 (1989).

[5] H. J. Mamin, M. Poggio, C. L. Degen, and D. Rugar. Nuclear magnetic resonance imaging with 90-nm resolution. *Nature Nanotechnology,* 2, 301 (2007).

[6] V. Pizzella S. Della Penna, C. Del Gratta, and G. L. Romani. SQUID systems for biomagnetic imaging. *Superconductor Science and Technology,* 14, R79 (2001).

[7] A. M. Chang, H. D. Hallen, L. Harriott, H. F. Hess, H. L. Kao, J. Kwo, R. E. Miller, R. Wolfe. Scanning Hall probe microscopy. *Applied Physics Letters,* Vol. 61, pp. 1974 (1992).

[8] H. B. Dang, A. C. Maloof, and M. V. Romalis. Ultrahigh sensitivity magnetic field and magnetization measurements with an atomic magnetometer. *Applied Physics Letters* 97, 151110 (2010).

[9] J. M. Taylor, P. Cappellaro, L. Childress, L. Jiang, D. Budker, P. R. Hemmer, A. Yacoby, R. Walsworth, and M. D. Lukin. High-sensitivity diamond magnetometer with nanoscale resolution. *Nature Physics* 4, 810 (2008).

[10] M. Vengalattore, J. M. Higbie, S. R. Leslie, J. Guzman, L. E. Sadler, and D. M. Stamper-Kurn. High-resolution magnetometry with a spinor Bose-Einstein condensate. *Physical Review Letters* 98, 200801 (2007).

[11] M. V. Romalis, and H. B. Dang. Atomic magnetometers for materials characterization. *Materials Today* 14, 258 (2011).

[12] M. Sawicki, W. Stefanowicz and A. Ney. Sensitive SQUID magnetometry for studying nanomagnetism. *Semiconductor Science and Technology,* 26 064006 (2011).

[13] D. Maser, S. Pandey, Ring, M. P. Ledbetter, S. Knappe, J. Kitching, and D. Budker. Note: Detection of a single cobalt microparticle with a microfabricated atomic magnetometer. *Review of Scientific Instruments* , Vol. 82, p. 086112 (2011).

[14] D. Budker, and M. Romalis. Optical magnetometry. *Nature Physics,* 3, 227 (2007).

[15] G. Balasubramanian, P. Neumann, D. Twitchen, M. Markham, R. Kolesov, N. Mizuochi, J. Isoya, J. Achard, J. Beck, J. Tissler, V. Jacques, P. R. Hemmer, F. Jelezko and J. Wrachtrup. Ultralong spin coherence time in isotopically engineered diamond. *Nature Materials,* 8, 383 (2009).

[16] J. R. Maze, P. L. Stanwix, J. S. Hodges, S. Hong, J. M. Taylor, P. Cappellaro, L. Jiang, M. V. G. Dutt, E. Togan, A. S. Zibrov, A. Yacoby, R. L. Walsworth, and M. D. Lukin. Nanoscale magnetic sensing with an individual electronic spin in diamond. *Nature,* 455, 644-647 (2008).

[17] M. S. Grinolds, P. Maletinsky, S. Hong, M. D. Lukin, R. L. Walsworth, and A. Yacoby. Quantum control of proximal spins using nanoscale magnetic resonance imaging *Nature Physics,* 7, 687 (2011).

[18] L. M. Pham, D. Le Sage, P. L. Stanwix, T. K. Yeung, D. Glenn, A. Trifonov, P. Cappellaro, P. R. Hemmer, M. D. Lukin, H. Park, A. Yacoby and R. L. Walsworth. Magnetic field imaging with nitrogen-vacancy ensembles *New Journal of Physics,* 13 (2011).

[19] R. S. Schoenfeld, and W. Harneit. Real Time Magnetic Field Sensing and Imaging Using a Single Spin in Diamond. *Physical Review Letters,* 106, 030802 (2011).

[20] S. Xu, V. V. Yashchuk, M. H. Donaldson, S. M. Rochester, D. Budker, and A. Pines. Magnetic resonance imaging with an optical atomic magnetometer. *Proceedings of the National Academy of Sciences*, 103, 12668-12671 (2006).

[21] M. P. Ledbetter, T. Theis, J.W. Blanchard, H. Ring, P. Ganssle, S. Appelt, B. Blümich, A. Pines, and D. Budker. Near-Zero-Field Nuclear Magnetic Resonance. *Physical Review Letters,* 107, 107601 (2011).

[22] J. Jang, R. Budakian, and Y. Maeno. Phase-locked cantilever magnetometry. *Applied Physics Letters,* 98, 132510 (2011).

[23] L.-S. Bouchard, V. M. Acosta, E. Bauch and D. Budker. Detection of the Meissner effect with a diamond magnetometer. *New Journal of Physics,* 13 025017 (2011).

[24] M. Hämäläinen, R. Hari, R. J. Ilmoniemi, J. Knuutila, and O. V. Lounasmaa. Magnetoencephalography - theory, instrumentation, and applications to noninvasive studies of the working human brain. *Reviews of Modern Physics,* Vol. 65, No. 2, (1993).

[25] S. Palva and J. M. Palva. New vistas for α-frequency band oscillations. *Trends in Neurosciences,* 30, 150 (2007).

[26] S. Forstner, S. Prams, J. Knittel, E.D. van Ooijen, J.D. Swaim, G.I. Harris, A. Szorkovszky, W.P. Bowen, H. Rubinsztein-Dunlop. Cavity Optomechanical Magnetometer. *arXiv* 1110.2271v1 [physics.optics] (2011).

[27] T.J. Kippenberg and K.J. Vahala. Cavity Optomechanics: Back-Action at the Mesoscale. *Science* 321, 1172 (2008).

[28] T. Corbitt and N. Mavalvala. Quantum noise in gravitational-wave interferometers. *Journal of Optics B: Quantum and Semiclassical Optics,*

[29] K. H. Lee, T. G. McRae, G. I. Harris, J. Knittel, and W. P. Bowen. Cooling and control of a cavity optoelectromechanical system. *Physical Review Letters,* 104 123604 (2010).

[30] A Schliesser, G Anetsberger, R Riviere, O Arcizet, and T J Kippenberg. High-sensitivity monitoring of micromechanical vibration using optical whispering gallery mode resonators. *New Journal of Physics,* 10, 095015 (2008).

[31] C.A. Regal, J. D. Teufel, and K. W. Lehnert. Measuring nanomechanical motion with a microwave cavity interferometer. *Nature Physics* 4, 555 - 560 (2008).

[32] A. H. Safavi-Naeini, J. Chan, J. T. Hill, T. P. M. Alegre, A. Krause, and O. Painter. Measurement of the quantum zero-point motion of a nanomechanical resonator. *arXiv,* 1108.4680v1 [quant-ph] (2011).

[33] J. Chan, T. P. M. Alegre, A. H. Safavi-Naeini, J. T. Hill, A. Krause, S. Grblacher, M. Aspelmeyer, and O. Painter. Laser cooling of a nanomechanical oscillator into its quantum ground state

[34] J. Liu, K. Usami, A. Naesby, T. Bagci, E. S. Polzik, P. Lodahl, and S. Stobbe. High-Q optomechanical GaAs nanomembranes. *arXiv,* 1110.1618v2 [cond-mat.mes-hall] (2011).

[35] H. Cai and A. W. Poon. Optical manipulation of microparticles using whispering-gallery modes in a silicon nitride microdisk resonator. *Optics Letters* 36, 4257 (2011).

[36] C. P. Dietrich, M. Lange, C. Sturm, R. Schmidt-Grund and M. Grundmann. One- and two-dimensional cavity modes in ZnO microwires. *New Journal of Physics,* 13, 103021 (2011).

[37] D. Kleckner, B. Pepper, E. Jeffrey, P. Sonin, S. M. Thon, and D. Bouwmeester. Optomechanical trampoline resonators. *Optics Express,* 19, 19708 (2011).

[38] A. G. Kuhn, M. Bahriz, O. Ducloux, C. Chartier, O. Le Traon, T. Briant, P.-F. Cohadon, A. Heidmann, C. Michel, L. Pinard, and R. Flaminio. A micropillar for cavity optomechanics. *Applied Physics Letters,* 99, 121103 (2011).

[39] I. Wilson-Rae, C. Galland, W. Zwerger, and A. Imamoglu. Nano-optomechanics with localized carbon-nanotube excitons. *arXiv,* 0911.1330v1 [cond-mat.mes-hall] (2009).

[40] L. D. Landau and E. M. Lifshitz. *Theory of elasticity* Course of Theoretical Physics v.7. Pergamon Press, 2nd edition (1970).

[41] Terry G. McRae and Warwick P. Bowen. Near threshold all-optical backaction amplifier. *arXiv* 1109.2004v1 [quant-ph] (2011).